Journal of Robotics and Control (JRC)
Volume 5, Issue 3, 2024
ISSN: 2715-5072, DOI: 10.18196/jrc.v5i3.21614

System Identification and Control Strategy on Electric Power Steering DC Motor

Bustanul Arifin [1*], Agus Adhi Nugroho [2], Eka Nuryanto Budisusila [3], Muhammad Khosyi'in [4]
[1, 2, 3, 4] Department of Electrical Engineering, Universitas Islam Sultan Agung, Semarang, Indonesia
Email: [1] bustanul@unissula.ac.id, [2] agusadhi@unissula.ac.id, [3] ekanbs@unissula.ac.id, [4] chosy@unissula.ac.id
*Corresponding Author

***Abstract*—Power steering technology help human to control the car. The hydraulic power steering system now tends to be replaced by the electric power steering system (EPS). As the main driver that require precise control. The contribution of this research is to obtain system identification of EPS motor and novelty control strategy to achieve stable control better. Motor control require an appropriate mathematical model and up-down-up down signals of Pseudo Random Binary Signal Sequence (PRBS) were used. The modelling method used was the Numerical Algorithm for Subspace State Space System Identification (N4SID). The quality of the modeling needs to be measured to see whether it was close to the original signal. The validation of the model obtained tested using Variance Accounted For (VAC), Akaike Information Criterion (AIC), and Final Prediction Error (FPE). The best mathematical model was developed on the basis of these three criteria, which is 3rd order model. The control strategy carried out by means of the Ziegler Nichols, Tyreus Luyben and Haugen tuning technique. With these three tuning methods, the control parameters obtained were used for Proprotional-Integral (PI) and Proportional-Integral-Derivative (PID) control. Based on the study, the Haugen control shows the best results of the two other controls, namely with a rise time value of 11.361 ms, overshoot of 6.898%, and steady state at 1.3 s. This show that PI control using the Haugen tuning method able to control the motor well. Robustness tests have also been carried out because the steering system is operated in unpredictable environmental conditions. The control greatly influenced the performance and stability of EPS control in the car's steering system.**

Keywords—System Identification; EPS DC Motor; Myrio1900; Tuning Method; Performance; Stability.

I. INTRODUCTION

The driver has to control the car to regulate the speed and direction of steering movement. Originally, the steering system directly connected the steering column to the wheels which supported the weight of the entire vehicle. As the load of a car increased, conventional steering is rarely found due to several weaknesses. Evolution of the steering system from previously refined conventional systems to hydraulic steering systems. With hydraulic pressure obtained from a pump connected to the engine, the Hydraulic Power Steering (HPS) system helps lighten the steering load. Some of the developments in the HPS study are the analysis of the geometric relationship between the response characteristics and the spool edge of the power steering gear valve [1], analysis of hydraulic pressure and load, steering angle, angular speed using the K-means clustering method was used for light vehicle steering systems [2], and for wheel loader on performance optimization development [3]. The HPS system was perfected by using the Electric Hydraulic Power Steering (EHPS) system which was a combination of a hydraulic system and an electric system. The research that developed the system was regulating motor rotor speed control to improve power control [4], and the estimated uncertainty model was used to control EHPS in the context of stability and robust performance testing [5]. However, improvements to the EHPS system still have weaknesses, including the fact that it still uses a hydraulic system which requires replacement of the fluid system and was a complex system. The final refinement of the steering system was EPS which uses pure electricity to lighten the car's steering. Study was conducted to improves steering feel with an algorithm based on a mathematical model of the steering system's steering torque [6], utilization of neural networks to improve steering wheel torque performance [7], and to increase stability and robustness in EPS steering with the Linear Quadratic Gaussian algorithm [8]. The main component of EPS is the motor. Motors as plants were used for various types of steering control, including Permanent Magnet Synchronous (PMS) motor [9], Consequent-Pole Permanent Magnet motor [10][11], Brushless Direct Current (BLDC) motor [12]. DC EPS motors are rarely used for studies because of their availability in car steering systems in different regions.

To obtain a good control system in according to its purpose, an in-depth analysis of the plant is required. The analysis was obtained from the physical model of the plant which was a mathematical model [13]–[16]. As a result, the role of mathematical models was very important in control. There are two ways to obtain parameter values for a plant into a mathematical model, including direct measurement and system identification. Measurement carried out to obtain the moment of inertia value [17], torque of small motor [18], torque of spherical moto r[19], inductance stepper motor [20], electric resistance and dynamic self mutual inductions motor [21]. System identification using mathematic modelling for swithced reluctance motor [22], torque modelling [23], vane air motor [24], motor loss distribution [25]. Measurement of parameters at the plant requires measuring equipment/instrumentation tools with high accuracy to get accurate and precise values. Beside that, the difficulty in accessing the plant to take measurements is a weakness of this method. The use of identification systems was an alternative that can be taken to overcome the limitations of direct parameter measurement [26]–[28].

There are many challenges in identifying the parameters of a plant. These challenges can be seen from the

experimental design to the model development stage. To create a comprehensive model and system identification, linear models, discrete models and least squares parameter estimation were used [29], runge-kutta 4 for the recursive filter method [30], the recursive least squares (RLS) algorithm was used in finding induction motor parameters [31]. The fractional differential equation has been proven to also be able to find induction motor parameters both through simulation and experiment [32], identification for monitoring of electromechanical oscillations solved by N4SID [33].

In recent years, proportional-integral-derivative (PID) control has been developed in several studies. PID control has several advantages over other controls and can produce a satisfactory control system [34]. The control was also applied to DC motor control with open loop and closed loop systems [35], [36]. Closed loop control has the advantage of improving control performance well due to error correction from the feedback [37]. Tuning methods to obtain PID control parameters generally use the Ziegler Nichols method, both open loop [38] and closed loop [39] methods.

The paper introduce the system identification subspace method used to obtain the mathematical modeling of DC EPS motors. The main contribution of the research lies in a new approach to tuning strategies for DC EPS motor control. The control previously developed to only use one tuning. In comparison of three tunings carried out improve control. The research also contributes to improving DC motor control used in steering systems. The EPS DC motor of the Brio car with a specification of 2500 rpm which works at a voltage of 12 v was used as a plant. This motor was connected to an HN3806AB rotary encoder to count the number of revolutions produced. To obtain the motor modeling, the N4SID method was used with up and down signal input of the PRBS signal. myRIO board with LabVIEW software used to process data to produce the system model. To validate the model obtained, three parameters were used, namely VAC, AIC, and FPE so that the correct model was obtained. Furthermore, this modeling was tested three tuning methods for closed loop control systems. The three tuning methods were the Ziegler Nichols, Tyreus-Luyben, and Haugen methods. The proposed method aims to improve the efficiency and stability of steering operation. With these results, the level of safety and performance of car steering can be improved.

The structure of this article is: section II Research Method which consists of system modeling, Identification Algorithm, Experimental Setup, Controller Parameter Tuning. Section III Results and Discussions consists of System Identification, Control Method Comparison, Robustness Analysis, Discussion of Results. Section IV Conclusion of paper.

II. RESEARCH METHOD

A. System Modeling

Both state-space and transfer function models are a form of a dynamic model which can be called a black-box model [40]–[42]. The black-box model does not directly describe information about the system physically but rather describes the dynamic parameters of the system [43]–[45]. In this system, a continuous system is converted into a discrete system because it has advantages when used to estimate a system. This is because the incoming signal data will be sampled for this purpose. There are several methods to estimate the system and one of them is the sub-space method [46][47]. The form of the state-space model equation in discrete time is:

$$x(t_{k+1)} = Ax(t_k) + Bu(t_k) + Ke(t_k) \quad (1)$$

$$y(t_k) = Cx(t_k) + Du(t_k) + e(t_k) \quad (2)$$

where x (0) is the initial state, the known input vector is $u(t_k)$, the known output vector is $y(t_k)$, the noise vector is $e(t_k)$, A, B, C, D, K are the matrix coefficients. Whereas $x(t_k)$ is the state vector that will be searched for when the process occurs.

The u and y computations are obtained from the Z-transfer function in the state-space model. By decreasing equations (1) and (2), the output of $y(z)$ is obtained by the following equation:

$$H_{y,u}(z) = C(zI - A)^{-1}B + D \quad (3)$$

where I is the identity matrix which has dimensions with the matrix A.

Estimation is carried out on five existing matrices in equation (1) and (2). The five of them have a special standard form. Estimates of the initial state are obtained from the time-series of input u to output y. So that the transfer function is obtained using equation (3). The selection of the order needs to be considered in order to get the right estimation results.

Selection of the right estimation model with a number of different parameters needs to be done carefully. According to the the Parsimony Principle [48]–[50], it is stated that among a number of appropriate models, the simplest model should be chosen. For a good model the smallest value should be chosen for Akaike Information Criterion (AIC) [51][52] equation (4) and Final Prediction Error (FPE) [53][54] equation (6).

$$AIC = log\left(J + \left(1 + \frac{2d}{N}\right)\right) \quad (4)$$

where d is the number of parameters estimated, and J is

$$J = \det\left(\frac{\varepsilon^T \varepsilon}{N}\right) \quad (5)$$

where ε is the prediction error vector, that is, the reduction in the output vector actual system with the predicted model output vector, and N is amount of data.

$$FPE = J\left(\frac{1 + \frac{d}{N}}{1 - \frac{d}{N}}\right) \quad (6)$$

B. Identification Algorithm

System identification methods divided into two, including the classical and subspace methods. In the subspace method in Fig. 1, first constructs a state estimate from the given input-output data using a simple procedure based on numerical linear algebra tools. The state space model is obtained by solving the least squares problem for which we can easily calculate the transfer matrix if necessary. the important thing of the study of subspace methods is to understand the key point how Kalman filters state vectors and extended observability matrices obtained using algebraic numerical linear tools.

The subspace method has the advantage that it is based on reliable numerical algorithms of QR decomposition and singular value decomposition (SVD). QR decomposition (QR factorization) is the decomposition of matrix A into the product A = QR of the orthonormal matrix Q and the upper triangular matrix R. LQ decomposition is the lower triangular matrix L. SVD of a matrix is the factorization of the matrix into three matrices [55]. With these two decompositions, there is no need for optimization techniques (nonlinear) and the application of canonical form to the system. This implies that subspace algorithms can also be applied to multiple-input multiple-output as well as single-input single-output system identification.

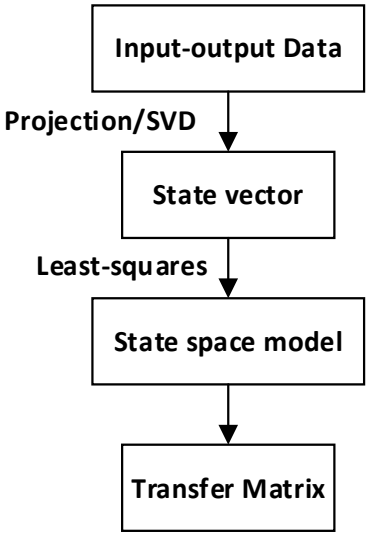

Fig. 1. Subspace method of system identification

One of the subspace methods is N4SID. N4SID algorithm can be done as follows [33][56][57]:

1. Calculates LQ decomposition of U_p, U_f, Y_p, Y_f from the equation (7). While L shows the lower triangular matrix L for LQ decomposition [58].

$$\begin{bmatrix} U_f \\ U_p \\ Y_p \\ Y_f \end{bmatrix} = \begin{bmatrix} L_{11} & 0 & 0 & 0 \\ L_{21} & L_{22} & 0 & 0 \\ L_{31} & L_{32} & L_{33} & 0 \\ L_{41} & L_{42} & L_{43} & L_{44} \end{bmatrix} \begin{bmatrix} Q_1^T \\ Q_2^T \\ Q_3^T \\ Q_4^T \end{bmatrix} \quad (7)$$

Since $L_{44} = 0$, the future Y_f is completely determined by the pas W_p and the future inputs U_f. Equation (7) can be simplified to be

$$\begin{bmatrix} U_f \\ W_p \\ Y_f \end{bmatrix} = \begin{bmatrix} R_{11} & 0 & 0 \\ R_{21} & R_{22} & 0 \\ R_{31} & R_{32} & 0 \end{bmatrix} \begin{bmatrix} Q_1^T \\ Q_2^T \\ Q_3^T \end{bmatrix} \quad (8)$$

2. Determine the value ξ from equation (9).

$$e = \hat{E}_{||U_f}\{Y_f|W_p\} = R_{32}R_{22}^{\dagger}W_p = \mathcal{O}_k X_f \quad (9)$$

3. Calculates ξ matrices using the SVD decomposition of the equation (10).

$$\xi = (U_1 \quad U_2)\begin{pmatrix} S_1 & 0 & 0 \\ 0 & \ddots & 0 \\ 0 & 0 & S_i \end{pmatrix}\begin{pmatrix} V_1^T \\ V_2^T \end{pmatrix} \quad (10)$$

4. Determine the value of $\mathcal{O}_k$ to get the parameters of matrices A and C

5. Determine the value of the matrix B and C using equation (11) and (12).

$$\Psi_k = \left(R_{31} - R_{32}R_{22}^{\dagger}W_p\right)R_{11}^{-1} \quad (11)$$

$$\Psi_k = \begin{bmatrix} D & 0 & \cdots & 0 \\ CB & D & \cdots & 0 \\ \vdots & \vdots & \ddots & \vdots \\ CA^{k-2}B & CA^{k-3}B & \ldots & D \end{bmatrix} \quad (12)$$

C. Experimental Setup

The flowchart of this research is shown in Fig. 2. For system modelling purposes, some good signals for this process are PRBS signal, chirp signal, up-down-up signal [59]–[62]. The initial step this research was collecting the data to be processed. The selected signal was an up-down-up signal which will go through a filtering process to reduce noise.

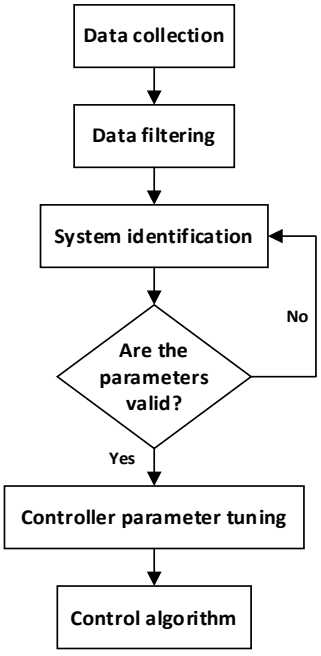

Fig. 2. Flowchart of method research

The signal was divided into two, the first signal was for estimation and the second signal was used for testing purposes. The first half signal was used for estimation input to obtain a mathematical model. To test the results of the mathematical model, the second half of the signal was used. Testing checks whether the resulting signal was similar to the original signal. The identification system used the N4SID method which has been described previously and its validation will be tested to see whether the resulting parameters were valid. Validation testing uses VAC, AIC, and FPE. If the results were valid then the next step was tuning the control parameters. Conversely, if it was invalid, the process will be repeated. The three tuning methods used for research were the Ziegler Nichols, Tyreus-Luyben, and Haugen methods. By comparing the responses obtained from the three, the appropriate control was selected to be used for the DC EPS motor control algorithm.

Fig. 3 shows block diagram of this research. The system identification consists of a computer, myRIO 1900 board, motor driver, DC EPS motor, rotary encoder, and several measuring instruments. myRIO 1900 board was used as the main microprocessor system in this study. Up-down-up signal were generated by myRIO board. The main processor was Xilink Z-7010 with a speed of 667 MHz. The board has 512 MB no volatile memory and 256 MB DDR3 memory. The board has a 14-pin digital input output with a 40 kiloohm pullup resistor on a voltage of 3.3 V and 6 analog input outputs. myRIO board's analog output was 100 mA so a driver was required to activate the motor. The driver connected to the output of this board was BTS7960. This driver uses MOSFET with a PWM capacity of 25 KHz with an output current of 43 A. As plant, the DC EPS motor has a rotation of 2500 rpm at a voltage of 12 V. The motor shaft was connected to a rotary encoder which functions to calculate the motor rotation. The rotary encoder used was HN3806AB with NPN open collector output specifications. The device works at a frequency of 30 KHz. The rotary encoder output was connected to the road myRIO which was equipped with an identification program. The hardware arrangement used in this research is as shown in Fig. 4.

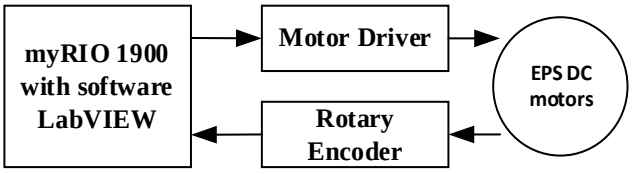

Fig. 3. Block diagram of system identification

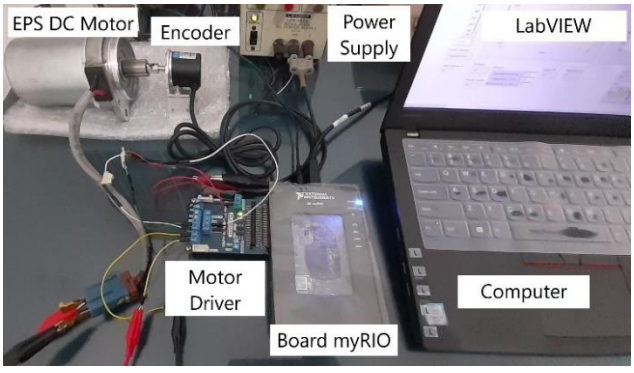

Fig. 4. Hardware diagram of system identification

The software board platform was the Laboratory Virtual Instrument Engineering Workbench (LabVIEW) made by National Instruments which is compatible with myRIO hardware. With an image/visual based programming system, the system identification is shown in Fig. 5.

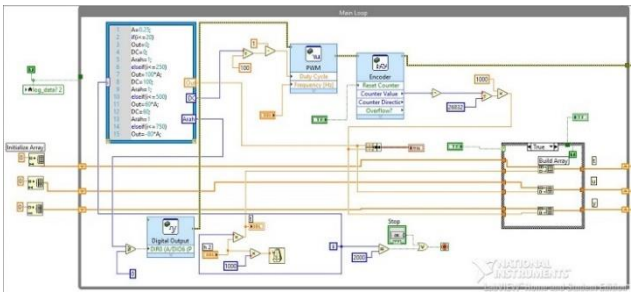

Fig. 5. LabVIEW programming of motor system identification

D. Controller Parameter Tuning

The automatic controller calculates the divergence between the actual and desired values of the plant output and then sends out a control signal to minimize the deviation to either zero or a minor value. A control signal known as a control action is produced by the automatic control mode. A closed loop control system is used to reduce overshoot or undershoot that occur when disturbances occur [63], as well as good system response due to faster feedback [64].

PID control offers a number of benefits. Essentially, proportional control (P) is an amplifier with tunable gain. This control will enhance overshoot, decrease steady state errors, and shorten the rise time. While removing steady state faults, integral control (I) will lead to a subpar transient response. Derivative control (D) will, in the meantime, improve transfer response, decrease overshoot, and increase system stability [65]–[68].

The Ziegler-Nichols approach can be used to derive PID control values [69][70]. The output of the system was connected to the input, therefore this method was called a closed loop method. At that time, the gain was increased continuously so that the output produces an oscillating signal [71][72]. The resulting period was called Pu, and the critical value of maximum gain was called ultimate gain (Kcr). With Kcu being the gain that produces oscillations and Pu was the resulting period, the values of the PID control parameters are obtained based on Table I.

TABLE I. ZIEGLER NICHOLS PARAMETERS

Control Type	Parameter		
	K_p	T_i	T_d
PI	0.45 Kcr	0.83 Pu	0
PID	0.6 Kcr	0.5 Pu	0.125 Pu

Tuning with the Tyreus-Luyben method still uses the basic Ziegler Nichols tuning [73]–[75]. The difference in this method is the parameters used as shown in Table II.

TABLE II. TYREUS-LUYBEN PARAMETERS

Control Type	Parameter		
	K_p	T_i	T_d
PI	0.31 Kcr	2.2 Pu	0
PID	0.45 Kcr	2.2 Pu	0.158 Pu

The third tuning method that has been used in this study was the Good Gain method developed by Finn Haugen. By arranging the control in a closed loop that has an input step and a gain. This gain value was increased continuously until it reaches KpGG gain which results in an output signal that has overshoot and undershoot [76]. The time generated between overshoot and undershoot was called Tou. The parameters for the PID tuning of the Good Gain method are shown in Table III.

TABLE III. HAUGEN PARAMETERS

Control Type	Parameter		
	K_p	T_i	T_d
PI	0.8 Kcr	1.5 Pu	0
PID	0.8 Kcr	1.5 Pu	0.25 Pu

III. RESULT AND DISCUSSION

A. System Identification

There were two important steps taken to implement the identification system. The first was recording output data based on input respons and the second was the identification process itself. The red line in Fig. 6 is the up-down-up signal input to the motor, while the blue line represents the motor response obtained from data collection in the rotary encoder. Positive and negative Rpm indicates that the motor was rotating in the opposite direction. It can be seen that the motor could not reach the desired RPM value due to motor resistance and delay time. And this was a normal phenomenon.

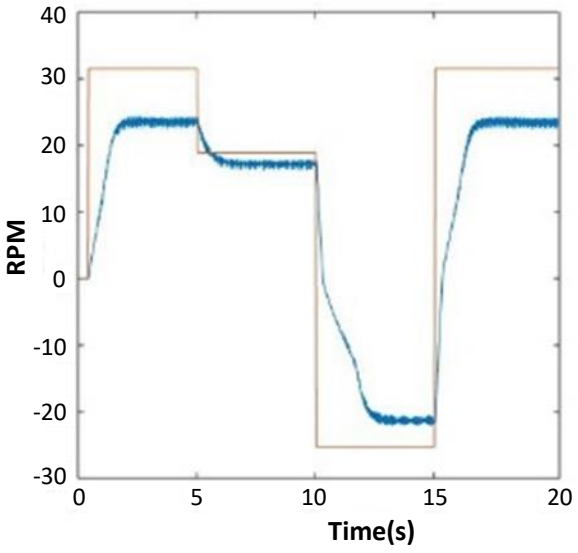

Fig. 6. Input-output signal for collecting data

The sampling interval used for this identification process was 0.02 seconds. Input data (red line) and output data (blue line) were processed by myRIO. The N4SID identification system was implemented based on the data that has been collected. This process produces 1st to 3rd order mathematical modeling. System identification used the measurement data that the process provides to estimate the unknown parameters of the model under a specific error criteria [77]. VAC, AIC, or FPE can be used to identify the proper model sequence. Table IV shows the parameter values for 1st to 3rd order. To get good results, choose a model that has a large VAF value and a small AIC and FPE value [51]–[54]. By looking at Table IV it was known that the VAF values for 1st order and 3rd order were almost similar but slightly superior for 3rd order. Meanwhile, the value of AIC third order was smaller than 1st order and 2nd order. For the FPE value, the smallest value was obtained in the equation with 1st order, followed by 3rd order, and finally 2d order. With these considerations, the 3rd order model was chosen.

TABLE IV. VAIC, AIC, AND FPE PARAMETERS

Order	Parameter		
	VAF	*AIC*	*FPE*
1st	94.8190	2.9248	17.7634
2nd	94.0640	3.0613	20.7050
3rd	94.8512	2.9206	18.0900

The resulting transfer function with the 3rd order was. Fig. 7 shows three signals including the input signal (pink line), the estimation signal (red line), and the response signal from the motor (blue line). It can be seen that the input signal was not completely achieved by the estimation signal. This was due to the data collection process in Fig. 6 with the arguments explained previously. The most important thing was that the estimation signal and the motor response signal were similar. There was a striking difference between these two signals at the initial time, but this phenomenon was acceptable because the motor requires a delay time and rise time to reach the desired signal. In fact, these parameters related to motor response were the subject of discussion in the following research.

$$\frac{1.26\,s^2 + 27.86\,s + 52734.82}{1.47\,s^3 + 112.27\,s^2 + 38552.43\,s + 50915.38} \quad (13)$$

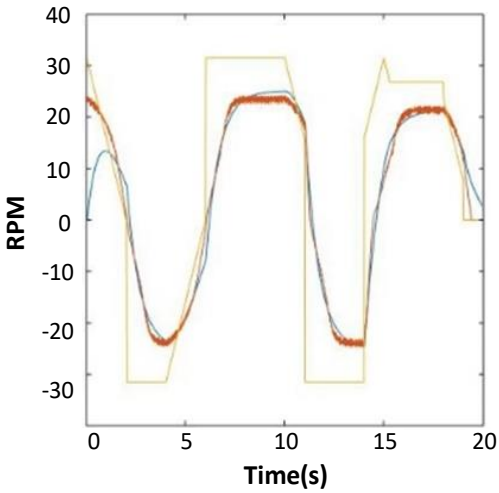

Fig. 7. Estimation signal and real signal

B. Control Method Comparison

The mathematical model in equation (13) of the system will be used as a plant to be given PI and PID control. This control was chosen because of its reliability and simplicity which only controls three parameters including K_p, T_i, and T_d [78].

Based on the root locus calculation as shown in Fig. 8, it showed that the EPS DC motor system has complex conjugation poles, so the best approach was to use a closed-loop system. The resulting equation (13) was stable because the roots of the characteristic equation were all negative.

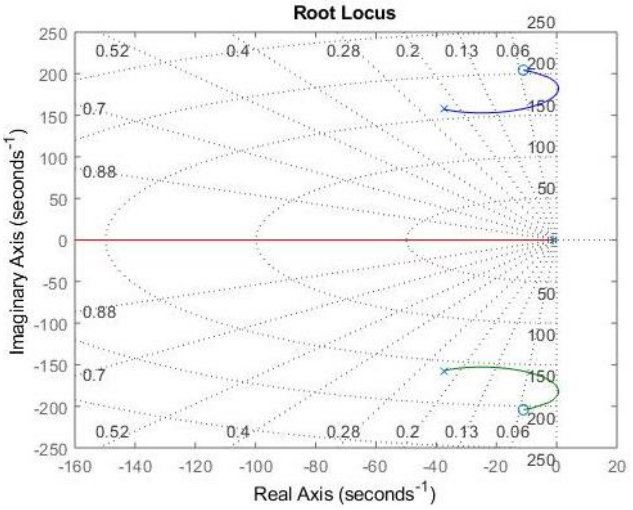

Fig. 8. Root locus of EPS DC motor system

An unstable system occurred when the response to an input produces loud oscillations at a certain amplitude. Whereas the system was stable if the system will remain in a stationary state or stop unless stimulated (excited by an input function and will return to rest if the excitation was eliminated). A stable system response can be seen from the transition that decreases towards zero with increasing time. To determine whether a system was stable or not, several methods were used, including Nyquist criteria and Bode criteria [79].

The Nyquist stability criterion was a criterion that relates the open loop frequency range $G\ (j\omega)\ H\ (j\omega)$ with a zero angle of $1\ +\ G\ (j\omega)\ H\ (j\omega)$ which lies to the right of the midwife s imaginary axis [80]. This criterion was very useful because the absolute stability of a closed loop system can be determined from the open loop frequency response curve so that there was no need to look for closed circular poles [81]. From equation (13) obtained by using the Nyquist stability analysis, a stable system with k values in the range of 486.2342 <k<Inf and -0.9655 <k<249.1969 was obtained.

The second criterion that can be used for stability was the Bode stability criterion. The closed loop system will be stable if and only if the magnitude of the open loop system was less than 1 at a frequency with a phase angle of 1800. Mathematically the Bode stability criteria were expressed in the equation:

$$|L(j\omega)| < 1 \tag{14}$$

where ω_180 was the crossover phase frequency. The results obtained with the stability criteria of the Bode system were declared stable at a value of K = 0.0040.

To obtain the robustness analysis, the maximum peak criterion value was used, where the criterion value was divided into two parts, namely the maximum peak sensitivity value and the maximum peak value of complementary sensitivity [82]. The maximum peak sensitivity value is obtained from equation (15) and the maximum peak value of complementary sensitivity in equation (16)

$$M_s = max_\omega |S(j\omega)| \tag{15}$$

$$M_T = max_\omega |T(j\omega)| \tag{16}$$

Based on the transfer function obtained in equation (13), the maximum peak criterion value for the sensitivity function was 1.0085 and the maximum peak criterion value for the complementary sensitivity function was 0.5088.

Margin of gain was the reciprocal of $|G(j\omega)|$ at the frequency where the phase angle was 1800. The frequency at which the phase angle was 1800 was known as the phase crossover frequency (ω_1) so that the gain margin (K_g) was expressed in terms of equation (17). Phase margin was the number of remaining phases added to the desired crossover gain frequency so that the system borders on an unstable state. Based on equation (13), the gain margin value was Gm = 44.1 dB with the gain margin frequency at 165 rad/s. While the value of the phase margin obtained was Pm = 165 dB at the phase margin frequency of 0.358 rad/s. Fig. 9 shows the Bode diagram of equation (13).

$$K_g = \frac{1}{|G(j\omega)|} \tag{17}$$

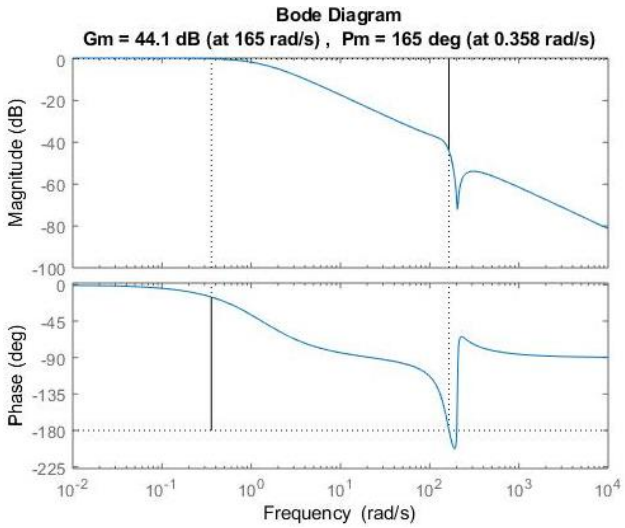

Fig. 9. Bode doagram EPS DC motor

The amplification that produces an oscillating output signal was worth 249.8632 and the required period of time was 0.035704 s. The reinforcement value was Kcr and the period was Pu entered in Table II to obtain the required control value. Table V summarizes the K_p, T_i, and T_d control values for PID control.

TABLE V. RESULT OF ZIEGLER-NICHOLS PARAMETER

Control Type	Parameter		
	K_p	T_i	T_d
PI	9.4233	0.0564	0
PID	12.3536	0.0340	0.0082

In this work, the EPS DC motor was controlled using a comparison of PI and PID control. Integral proportional control based on Table V produced K_p values of 9.4223 and T_i 0.0564. While PID control had parameters K_p = 12.3536, T_i = 0.0340, and T_d = 0.0082. Based on the parameter, rise time, overshoot, settling time, and stability criteria can be obtained. For the purpose of control design, these parameters were very essensial [83]. Fig. 10 illustrate the PI (red line) and PID (blue line) control response signal using Ziegler Nichols.

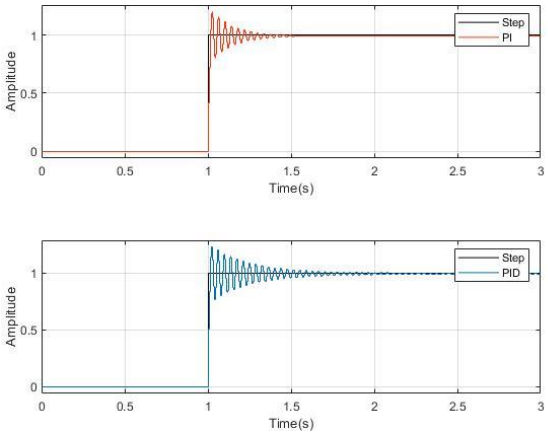

Fig. 10. System response of PI and PID control using Ziegler-Nichols

The rise time value for PI control was 18.736 ms with a peak amplitude of 1.198 at 1.025 ms. The overshoot value reached 21.34% and the slew rate was at 59.626/s. A stable value of 0.9915 was achieved at 1.306 s. All values are shown in Fig. 10 at the top (red line). This control has benefit was that it raised the final value to the intended set point by increasing the integral in the system.

In this investigation, complete controls P, I, and D were used. The peak amplitude value was obtained at the point of 1.227 at 1.023 s. The overshoot value generated by this control was slightly greater than the PI control, which was equal to 24.375%. Rise time generated in this control was worth 18.753 ms slightly smaller than the PI control. The resulting slewrate at a value of 69.106/s was greater than the PI control slew rate. This PID control reached a stable value at 0.9935 at 2.268 s. As shown in Fig. 10 at the bottom (blue line), the output of the PID control still oscillates a little, even though it was very small.

The Tyreus-Luyben method was also applied to the models produced by this EPS DC motor identification system. This method was based on the Ziegler-Nichols method but with a slight difference in determining the values of K_p, T_I, and T_d. On the basis of Table II, the control values were obtained as shown in Table VI.

TABLE VI. RESULTS OF TYREUS-LUYBEN PARAMETERS

Control Type	Parameter		
	K_p	T_i	T_d
PI	77.4576	0.07855	0
PID	147.4193	0.07855	0.005641

With Kp values of 77.4576 and Ti 0.07855 for PI control, and for PID control with K_p values of 147.4193, T_i 0.07855, and T_d 0.005641. The signal in Fig. 11 above (red line) was a response signal to the step signal that enters the input. The amplitude value that occurs was 1.125 at 1.028 s. The resulting rise time was 16.089 ms with a slew rate of 48.685/s. The overshoot that occured in this PI control was 14.368%. The stable value at 0.9888 occurred at 1.386 s.

The response signal to the PID control was shown in Fig. 11 below (blue line). The overshoot that occurred was 21.341% with a peak value of 1.195 amplitude at 1.026 s. The value of rise time on this signal was 13.139 ms with a slew rate of 59.650/s. The final signal oscillates slightly but was very small at values between 0.985 and 0.997 ranging from 1.477 s.

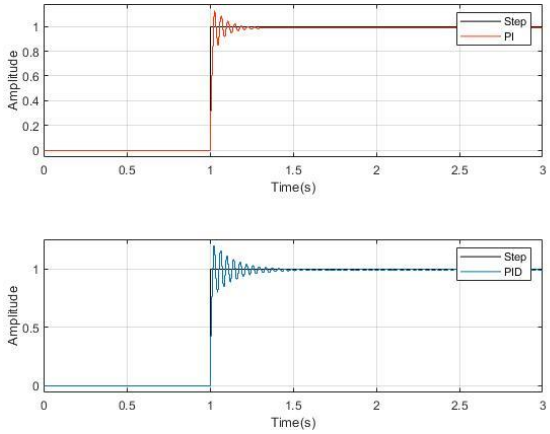

Fig. 11. System response of PI and PID control using Tyreus-Luyben

The method that has been used in this study was the Haugen method which was also known as the Good Gain method. The gain obtained when the response signal produces overshoot and undershoot was 75. From the output signal, the value between overshoot and undershoot was 18.554 ms. This value was used to obtain the control parameter values according to Table III. The control values of K_p, T_i, and T_d for the Haugen method were shown in Table VII.

TABLE VII. RESULTS OF HAUGEN PARAMETERS

Control Type	Parameter		
	Kp	*Ti*	*Td*
PI	60	0.0278	0
PID	60	0.0278	0.0069

Fig. 12 illustrates the control response signal of the PI, (red line) and PID (blue line) using the Haugen method. For PI control with K_p 60 and T_i 0.02782. While PID control with K_p 60, T_i 0.02782, and T_d 0.0069.

As shown in the Fig. 12 at the top (red line), the signal peak under PI control was 1.055 at 1.030 s with a rise time of 11.361 ms. The slew rate of this signal was 41.9/s and the overshoot was 6.989%. A value of 9.842 occurred at 1.3 s with a slight oscillation. The PID control illustrates in Figure 10 below (blue line) reached a peak amplitude of 1.051 at 1.030 s. The rise time that occurs was slightly smaller than the PI control, which was valued at 13.184 ms. The slew rate of this signal was 41.693/s. Signal overshoot with PID control reached 6.989%. A stable value of 0.9843 with a slight oscillation occurred starting at 1.3 s.

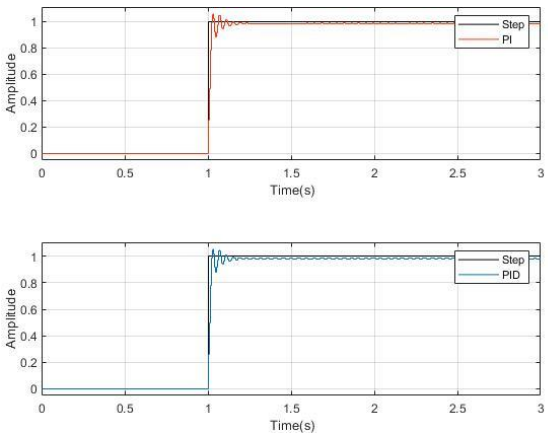

Fig. 12. System response of PI and PID control using Haugen

C. Robustness Analysis

Beside performance, the robustness of a system is also starting to be considered. Robustness of a system shows the system's ability to continue to provide the desired performance even though there were significant changes (uncertainties) in plant parameters [84]. The test is important because the DC EPS motor will be used for steering in changing road conditions.

To get a control robustness test, each control was given disturbances. The disturbance given to the system was in the form of a 10 ms impulse at 2s time with an amplitude of 50. Fig. 13 shows the results of the robustness test with disturbances in PI (blue line) and PID (red line) control using the Ziegler Nichols method. With PID control the signal would return to a stable state within 570 ms, while PID control takes a longer time, namely 720 ms to reach a stable point again. Even with PID control the signal still oscillated in small deviations.

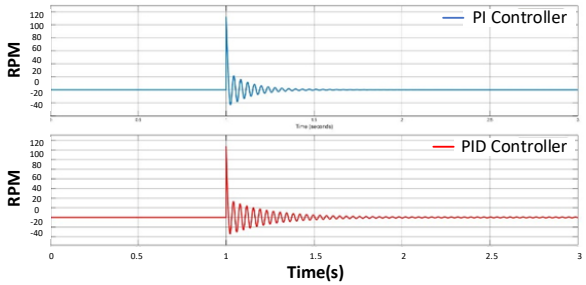

Fig. 13. Robustness test of control using Ziegler-Nichols

The robustness test of the Tyreus-Luyhen method controller was shown in Fig. 14. A stable state as before was obtained at 380 ms for PI control (blue line). Whereas for PID control (red line), a stable state was achieved at 510 ms.

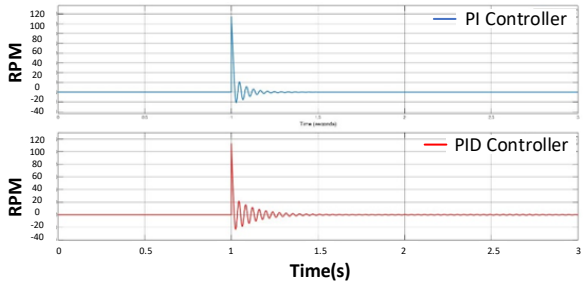

Fig. 14. Robustness test of control using Tyreus-Luyben

Similar to other methods, the Haugen method controller has also been tested for robustness. With the same noise signal as tested previously, the PI control (blue line) could return to a stable state at 260 ms. The time value of 270 ms was the time to stabilize the output signal after receiving interference for the PID method (red line). Fig. 15 illustrates the results of the signal getting interference for control by the Haugen method.

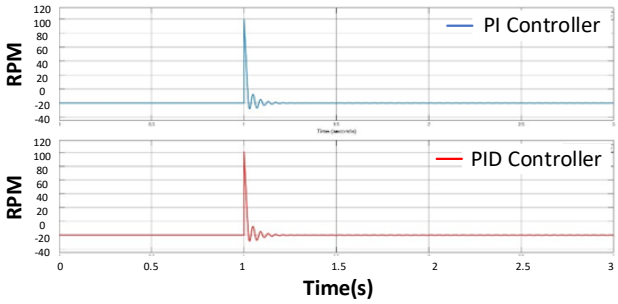

Fig. 15. Robustness test of control using Haugen

D. Discussion of Results

The aim of a control system is to adjust process variables to a desired state. Steering motor control requires precise and fast responses. The factor can be known from the rise time. Rise time was defined as the time it takes for a response to increase from 10% to 90% [85]. Based on the rise time value generated from the three controls, the smallest to largest values were the Haugen method, the Tyreus-Luyben method, and the Ziegler-Nichols method. From the definition, it means that the smallest rise time value was a good value for the control system. Therefore, the Haugen method control was a good control with the smallest time to achieve the desired value.

Overshoot was the maximum peak value of the response curve measured from unity. Therefore, overshoot was a performance indication that should not be ignored [86]. The steering control does not allow for overshoot or the tolerance was small. The Zeigler-Nichols method achieved the highest overshoot value, the second order was the Tyreus-Luyben method, and the smallest overshoot was achieved by control with the Haugen method. A proportional constant that was too large causes a large overshoot. However, with an appropriate combination of parameters, control with Haugen tuning can minimize overshoot.

Settling time was the time it takes for a response curve to reach and settle in the area around the final price whose size was determined by the absolute percentage of the final price (usually up to 5%)[87]. The Tyreus-Luyben method has the highest settling time value compared to the other two methods. The same value was obtained for the Ziegler-Nichols and Haugen controls, but the final value that was close to the steady state value was obtained by the control using the Ziegler-Nichols method.

The results of the system response showed that with the three methods used, PI control was better than PID control. In the Ziegler-Nichols method, the signal stabilizes faster with PI control than with PID control. Even in the PID control, it could be seen that the response signal still oscillates continuously even though it was in a small value. The same

phenomenon was shown in the Tyreus-Luyben control, where the signal with the PID control experiences a slowdown in achieving stability. The overshoot produced by this method was also higher than using the PI control. The results of the Haugen method control show that PI and PID control produced almost the same response signal between the two. This was understandable because of the use of similar formulas or equations. The value of rise time and overshoot between PI and PID controls with this method was only slightly different or can be said to be almost the same. But if it was seen from the resulting signal graph, it turns out that the PID control produces an oscillating signal too. So, it could be said that the results of the PI control signal were better because it was more stable than the PID control signal. PI control reliability was also strengthened when the system was disturbed. Based on the three methods, all of them show that the time to regain stability after being given a disturbance in the form of impulses with PI control ws smaller than that of PID control.

Compared with several other similar studies, this system offers significant improvement in terms of rise time and overshoot. Other studies used the trial and error [88] and the Ziegler Nichols tuning method without comparing other tuning methods [89]. In fact, Ziegler Nichols method was not always satisfactory for obtaining control parameters [90]. This research has proven that the proposed method was better than the method that has been widely used. The method was the Haugen method.

The strength of the research improves existing tuning methods. It can be seen that the Haugen method has advantages compared to the other two methods. The purpose was to increase the performance and stability of the DC motor in the steering system.

EPS DC motors were used for uncertain conditions. Uncertainty in the system occurs due to changes in plant parameters, plant dynamics that were not modeled, time delays that were not modeled, changes in the operating area, noise from sensors, disturbances that were not predicted. The last factor was often found in steering systems [91]. Another strength is that the research showed that disturbances that may occur on the highway can be reduced well with the proposed method.

Limitation of the study was that the reference value changes. The reason was that the car could experience changes in voltage due to an unstable electricity supply from a problematic accumulator. It was necessary to investigate whether this will significantly influence the rise time, overshoot and steady state values.

IV. CONCLUSION

The main objective of this study was to get an EPS DC motor system modeling and to find its control parameters. This was very important to do because the EPS system was used a lot in car steering systems, while the technical data for the motor was usually not available. By providing an input up-down-up signal to an EPS DC motor and investigating the response using N4SID method, system modeling could be obtained. This could be seen from the response of the simulation system close to the real system. The 3rd order mathematical model was obtained based on the validation of VAC, AIC, and FPE.

The control strategies chosen were PI and PID with three tuning methods including Ziegler Nichols, Tyreus-Lyuben, and Haugen. The rise time value was important because it shows how quickly the motor responds to steering. Among the three methods, the fastest was the Haugen method with PI control. Derivative parameters in PID control did not actually improve control results. The best results show that with PI control the Haugen method obtains rise time 11.361 ms and settling time at 1.3 s. Meanwhile, overshoot was 6.989%. This value could not be large because it will affect steering stability.

Highways are unpredictable conditions. Robustness testing needs to be carried out because the steering system will experience changing environmental conditions. The best results for this test were achieved by the Haugen method.

Based on these results, the main contribution of the research was demonstrated by a novelty EPS DC motor control method whose robustness has been tested. The control can improve the performance and stability of the steering system. Besides that, this control can also be developed for control purposes in industry.

Improved control can be tried further by using several other methods or algorithms. These algorithms include fuzzy logic control, neural networks, and other artificial intelligence algorithms. The control parameters investigated influence each other. The fuzzy method can increase rise time, reduce overshoot, and speed up steady state without affecting each other. The neural network training method can find the right control parameter values. This has the opportunity to get better control than the previous method. Robustness testing is related to DC motor voltage instability needs to be investigated more deeply.

ACKNOWLEDGMENT

Lembaga Penelitian dan Pengabdian Masyarakat Universitas Islam Sultan Agung (LPPM-Unissula).

REFERENCES

[1] C. Chen and Z. Li, "Research on Control and Optimization of Vehicle Steering Performance," *IEEE 6th Inf. Technol. Mechatronics Eng. Conf.*, pp. 2036–2039, 2022, doi: 10.1109/ITOEC53115.2022.9734596.

[2] S. E. Miri, M. Azadi, and S. Pakdel, "Development of a duty cycle with K-means clustering technique for hydraulic steering in an instrumented TIBA vehicle," *Transp. Eng.*, vol. 8, no. 100114, 2022, doi: 10.1016/j.treng.2022.100114.

[3] Y. Wang, X. Liu, J. Chen, W. Chen, C. Li, and D. Huo, "Design and control performance optimization of dual-mode hydraulic steering system for wheel loader," *Autom. Constr.*, vol. 143, no. 104539, 2022, doi: 10.1016/j.autcon.2022.104539.

[4] G. Geng, Q. Shen, and H. Jiang, "ANFTS Mode Control for an Electronically Controlled Hydraulic Power Steering System on a Permanent Magnet Slip Clutch," *Energies MDPI*, vol. 12, no. 9, 2019, doi: 10.3390/en12091739.

[5] A. Mitov, T. Slavov, and J. Kralev, "Robustness Analysis of an Electrohydraulic Steering Control System Based on the Estimated Uncertainty Model," *Inf. MDPI*, vol. 12, no. 12, 2021, doi: 10.3390/info12120512.

[6] J. H. Choi, K. Nam, and S. Oh, "Steering feel improvement by mathematical modeling of the Electric Power Steering system," *Mechatronics*, vol. 78, 2021, doi:

10.1016/j.mechatronics.2021.102629.

[7] S. You, G. Kim, S. Lee, D. Shin, and W. Kim, "Neural Approximation-Based Adaptive Control Using Reinforced Gain for Steering Wheel Torque Tracking of Electric Power Steering System," *EEE Trans. Syst. Man, Cybern. Syst.*, vol. 53, no. 7, pp. 4216–4225, 2023, doi: 10.1109/TSMC.2023.3241452.

[8] M. Irmer and H. Henrichfreise, "Design of a robust LQG Compensator for an Electric Power Steering," *IFAC-PapersOnLine*, vol. 53, no. 2, 2020, doi: 10.1016/j.ifacol.2020.12.082.

[9] H. Yang, S. Ademi, J. Paredes, and R. A. McMahon, "Comparative Study of Motor Topologies for Electric Power Steering System motor," *IEEE Work. Electr. Mach. Des. Control Diagnosis*, pp. 40-45, 2021, doi: 10.1109/WEMDCD51469.2021.9425673.

[10] Y. Tanaka, H. Minegishi, Y. Fujii, and A. Chiba, "Reduction of Torque Ripple and Radial Force Harmonics in Consequent-Pole Permanent Magnet Motor for Electric Power Steering Applications," *25th Int. Conf. Electr. Mach. Syst.*, pp. 1-6, 2022, doi: 10.1109/ICEMS56177.2022.9982893.

[11] S.-W. Song, M.-K. Hong, J. Lee, and W.-H. Kim, "A Study on Reduction of Cogging Torque and Magnet Usage through Intersect Magnet Consequent Pole Structure," *Energies*, vol. 15, no. 23, 2022, doi: 10.3390/en15239255.

[12] R. Manca *et al.*, "Performance Assessment of an Electric Power Steering System for Driverless Formula Student Vehicles," *Actuators*, vol. 10, no. 7, 2021, doi: 10.3390/act10070165.

[13] P. Thomas and P. K. Shanmugam, "A review on mathematical models of electric vehicle for energy management and grid integration studies," *J. Energy Storage*, vol. 55, p. 105468, 2022.

[14] L. Maybury, P. Corcoran, and L. Cipcigan, "Mathematical modelling of electric vehicle adoption: A systematic literature review," *Transp. Res. Part D Transp. Environ.*, vol. 107, 2022, doi: 10.1016/j.trd.2022.103278.

[15] M. Posypkin, A. Gorshenin, and V. Titarev, "Control, Optimization, and Mathematical Systems, Modeling of Complex," *Mathematics*, vol. 10, no. 13, 2022, doi: 10.3390/books978-3-0365-7641-1.

[16] K. Zimmermann, I. Zeidis, and V. Lysenko, "Mathematical model of a linear motor controlled by a periodic magnetic field considering dry and viscous friction," *Appl. Math. Model.*, vol. 89, no. 2, pp. 1155–1162, 2021, doi: 10.1016/j.apm.2020.08.021.

[17] A. Szántó, É. Ádámkó, G. Juhász, and G. Á. Sziki, "Simultaneous measurement of the moment of inertia and braking torque of electric motors applying additional inertia," *Meas. J. Int. Meas. Confed.*, vol. 204, 2022, doi: 10.1016/j.measurement.2022.112135.

[18] S. Pan, D. Wang, and W. Huang, "A novel small motor measurement system based on ultrasonic bearings," *Meas. J. Int. Meas. Confed.*, vol. 168, 2021, doi: 10.1016/j.measurement.2020.108307.

[19] Y. Wen, G. Li, Q. Wang, R. Tang, Y. Liu, and H. Li, "Investigation on the Measurement Method for Output Torque of a Spherical Motor," *Appl. Sci.*, vol. 10, no. 7, 2020, doi: 10.3390/app10072510.

[20] M. Akbaba and A. Dalcali, "A novel method for measuring inductances and analysis of shaded-pole motors," *Eng. Sci. Technol. an Int. J.*, vol. 36, 2022, doi: 10.1016/j.jestch.2022.101133.

[21] G. Á. Sziki, A. Szántó, J. Kiss, G. Juhász, and É. Ádámkó, "Measurement System for the Experimental Study and Testing of Electric Motors at the Faculty of Engineering, University of Debrecen," *Appl. Sci.*, vol. 12, no. 19, 2022, doi: 10.3390/app121910095.

[22] Z. Xu, C. Huang, H. Wang, D.-H. Lee, and F. Zhang, "Mathematical model of stepped rotor type 12/14 bearingless switched reluctance motor based on maxwell stress method," *Energy Reports*, vol. 9, no. 8, pp. 556–566, 2023, doi: 10.1016/j.egyr.2023.04.345.

[23] T. Zhang, G. Li, R. Zhou, Q. Wang, and L. Wang, "Torque Modeling of Reluctance Spherical Motors Using the Virtual Work Method," *Int. J. Appl. Electromagn. Mech.*, vol. 71, no. 3, pp. 199 – 219, 2023, doi: 10.3233/JAE-220104.

[24] V. I. Ivlev and S. Y. Misyurin, "Parameter identification for mathematical model of vane air motor," *Procedia Comput. Sci.*, vol. 213, pp. 240–249, 2022, doi: 10.1016/j.procs.2022.11.062.

[25] H. Shimoji, T. Ikeda, T. Todaka, S. Aihara, and K. Fujiwara, "Parameter identification for standardization of motor loss distribution measurement using thermographic camera," *J. Magn. Magn. Mater.*, vol. 591, p. 171694, 2024.

[26] B. Arifin, A. A. Nugroho, B. Suprapto, S. A. D. Prasetyowati, and Z. Nawawi, "Review of Method for System Identification on Motors," *Int. Conf. Electr. Eng. Comput. Sci. Informatics*, vol. 2021-Octob, no. October, pp. 257–262, 2021, doi: 10.23919/EECSI53397.2021.9624259.

[27] A. Ouannou, F. Giri, A. Brouri, H. Oubouaddi, and C. Abdelaali, "Parameter Identification of Switched Reluctance Motor Using Exponential Swept-Sine Signal," *IFAC-PapersOnLine*, vol. 55, no. 12, pp. 132–137, 2022, doi: 10.1016/j.ifacol.2022.07.300.

[28] S. Zhou, D. Wang, and Y. Li, "Parameter identification of permanent magnet synchronous motor based on modified- fuzzy particle swarm optimization," *Energy Reports*, vol. 9, no. 1, 2023, doi: 10.1016/j.egyr.2022.11.124.

[29] C.-C. Peng and C.-Y. Su, "Modeling and Parameter Identification of a Cooling Fan for Online Monitoring," *IEEE Trans. Instrum. Meas.*, vol. 70, pp. 1–14, 2021, doi: doi: 10.1109/TIM.2021.3104375.

[30] C.-C. Peng and T.-Y. Chen, "A recursive low-pass filtering method for a commercial cooling fan tray parameter online estimation with measurement noise," *Measurement*, vol. 205, 2022, doi: 10.1016/j.measurement.2022.112193.

[31] M. Nachtsheim, J. Ernst, C. Endisch, and R. Kennel, "Performance of Recursive Least Squares Algorithm Configurations for Online Parameter Identification of Induction Machines in an Automotive Environment," *IEEE Trans. Transp. Electrif.*, vol. 9, no. 3, pp. 4236–4254, 2023, doi: 10.1109/TTE.2023.3244619.

[32] V. A. Thomas and K. Srinivasan, "Design and implementation of enhanced PID controller in embedded platform for realtime applications," *2019 2nd Int. Conf. Power Embed. Drive Control (ICPEDC), Chennai, India*, pp. 129–133, 2019, doi: 10.1109/ICPEDC47771.2019.9036491.

[33] A. Zeno, M. Omtveit, and K. Uhlen, "Improvement of System Identification using N4SID and DBSCAN Clustering for Monitoring of Electromechanical Oscillations," *IEEE Belgrade PowerTech*, pp. 01-06, 2023, doi: 10.1109/PowerTech55446.2023.10202776.

[34] H. Q. T. Ngo, H. D. Nguven, and Q. V. Truong, "A Design of PID Controller Using FPGA-Realization for Motion Control Systems," *2020 Int. Conf. Adv. Comput. Appl. (ACOMP), Quy Nhon, Vietnam*, pp. 150–154, 2020, doi: 10.1109/ACOMP50827.2020.00030.

[35] D. C. Dursun, A. Yildiz, and M. Polat, "Modeling of Synchronous Reluctance Motor and Open and Closed Loop Speed Control," *2022 21st Int. Symp. INFOTEH-JAHORINA*, pp. 1-6, 2022, doi: 10.1109/INFOTEH53737.2022.9751332.

[36] M. K. Jayaram, "Analysis & Simulation of Open loop and Closed loop Control of a Flyback converter," *2022 Int. Conf. Electron. Renew. Syst.*, pp. 11–14, 2022, doi: 10.1109/ICEARS53579.2022.9752398.

[37] J. M. Diaz, R. Costa-Castello, and S. Dormido, "Closed-Loop Shaping Linear Control System Design: An Interactive Teaching/Learning Approach," *IEEE Control Syst. Mag.*, vol. 39, no. 5, pp. 58–74, 2019, doi: 10.1109/MCS.2019.2925255.

[38] C. S. Rao, S. Santosh, and D. R. V, "Tuning optimal PID controllers for open loop unstable first order plus time delay systems by minimizing ITAE criterion," *IFAC-PapersOnLine*, vol. 53, no. 1, pp. 123–128, 2020, doi: 10.1016/j.ifacol.2020.06.021.

[39] R. Aisuwarya and Y. Hidayati, "Implementation of Ziegler-Nichols PID Tuning Method on Stabilizing Temperature of Hot-water Dispenser," *2019 16th Int. Conf. Qual. Res. Int. Symp. Electr. Comput. Eng.*, pp. 1-5,2019, doi: 10.1109/QIR.2019.8898259.

[40] Y. Liang, S. Li, C. Yan, M. Li, and C. Jiang, "Explaining the black-box model: A survey of local interpretation methods for deep neural networks," *Neurocomputing*, vol. 419, pp. 168–182, 2021, doi: 10.1016/j.neucom.2020.08.011.

[41] L. Orellana, L. Sainz, E. Prieto-Araujo, M. Cheah-Mané, H. Mehrjerdi, and O. Gomis-Bellmunt, "Study of black-box models and participation factors for the Positive-Mode Damping stability criterion," *Int. J. Electr. Power Energy Syst.*, vol. 148, 2023, doi: 10.1016/j.ijepes.2023.108957.

[42] V. Anumola, C. P. R. Nadakuduru, and K. Vadde, "Implementation of Adaptive Cruise Control and Cloud based Black Box Technology for Modern Automotive Vehicles," *Int. Conf. Distrib. Comput. Electr. Circuits Electron.*, pp. 1–6, 2023, doi: 10.1109/ICDCECE57866.2023.10150905.

[43] O. Loyola-González, "Black-Box vs. White-Box: Understanding Their Advantages and Weaknesses From a Practical Point of View," *IEEE Access*, vol. 7, pp. 154096–154113, 2019, doi:

10.1109/ACCESS.2019.2949286.

[44] G. Rojas-Dueñas, J.-R. Riba, K. Kahalerras, M. Moreno-Eguilaz, A. Kadechk, and A. Gomez-Pau, "Black-Box Modelling of a DC-DC Buck Converter Based on a Recurrent Neural Network," *IEEE Int. Conf. Ind. Technol.*, pp. 456–461, 2020, doi: 10.1109/ICIT45562.2020.9067098.

[45] Y. Li, R. Lei, H. Hu, and K. Zhao, "A black box based model for phase change heat exchanger in refrigeration system simulations using Kriging interpolation method," *Int. J. Refrig.*, vol. 153, pp. 231–239, 2023, doi: 10.1016/j.ijrefrig.2023.05.005.

[46] İ. Uyanık, U. Saranlı, M. M. Ankaralı, N. J. Cowan, and Ö. Morgül, "Frequency-Domain Subspace Identification of Linear Time-Periodic (LTP) Systems," *IEEE Trans. Automat. Contr.*, vol. 64, no. 6, pp. 2529–2536, 2019, doi: 10.1109/TAC.2018.2867360.

[47] M. Yin, A. Iannelli, and R. S. Smith, "Subspace Identification of Linear Time-Periodic Systems With Periodic Inputs," *IEEE Control Syst. Lett.*, vol. 5, no. 1, pp. 145–150, 2021, doi: 10.1109/LCSYS.2020.3000950.

[48] A. A. Rohmawati and P. H. Gunawan, "The Causality Effect on Vector Autoregressive Model: The Case for Rainfall Forecasting," *2019 7th Int. Conf. Inf. Commun. Technol.*, pp. 1–5, 2019, doi: 10.1109/ICoICT.2019.8835379.

[49] L. Yang, H. Wang, Y. El-Laham, J. I. L. Fonte, D. T. Pérez, and M. F. Bugallo, "Indoor Altitude Estimation of Unmanned Aerial Vehicles Using a Bank of Kalman Filters," *ICASSP 2020 - 2020 IEEE Int. Conf. Acoust. Speech Signal Process.*, pp. 5455-5459, 2020, doi: 10.1109/ICASSP40776.2020.9054203.

[50] G. Brunetti, J. Šimůnek, D. Glöckler, and C. Stumpp, "Handling model complexity with parsimony: Numerical analysis of the nitrogen turnover in a controlled aquifer model setup," *J. Hydrol.*, vol. 584, 2020, doi: 10.1016/j.jhydrol.2020.124681.

[51] G. Flood-Page, L. Boutonnier, and J.-M. Pereira, "Application of the Akaike Information Criterion to the interpretation of bender element tests," *Soil Dyn. Earthq. Eng.*, vol. 177, 2024, doi: 10.1016/j.soildyn.2023.108373.

[52] M. Ingdal, R. Johnsen, and D. A. Harrington, "The Akaike information criterion in weighted regression of immittance data," *Electrochim. Acta*, vol. 317, pp. 648–653, 2019, doi: 10.1016/j.electacta.2019.06.030.

[53] G. Li, W. Chang, and H. Yang, "A Novel Combined Prediction Model for Monthly Mean Precipitation With Error Correction Strategy," *IEEE Access*, vol. 8, pp. 141432–141445, 2020, doi: 10.1109/ACCESS.2020.3013354.

[54] J.-U.-R. Chughtai, I. U. Haq, O. Shafiq, and M. Muneeb, "Travel Time Prediction Using Hybridized Deep Feature Space and Machine Learning Based Heterogeneous Ensemble," *IEEE Access*, vol. 10, pp. 98127–98139, 2022, doi: 10.1109/ACCESS.2022.3206384.

[55] S. Kaur and A. Jindal, "Singular Value Decomposition (SVD) based Image Tamper Detection Scheme," *2020 Int. Conf. Inven. Comput. Technol.*, 2020, doi: 10.1109/ICICT48043.2020.9112432.

[56] K. Li, H. Luo, C. Yang, and S. Yin, "Subspace-Aided Closed-Loop System Identification With Application to DC Motor System," *IEEE Trans. Ind. Electron.*, vol. 67, no. 3, pp. 2304–2313, 2020, doi: 10.1109/TIE.2019.2907447.

[57] C. M. Pappalardo, Ş. İ. Lök, L. Malgaca, and D. Guida, "Experimental modal analysis of a single-link flexible robotic manipulator with curved geometry using applied system identification methods," *Mech. Syst. Signal Process.*, vol. 200, 2023, doi: 10.1016/j.ymssp.2023.110629.

[58] S. N. Campelo, E. J. Jacobs IV, K. N. Aycock, and R. V. Davalos, "Real-Time Temperature Rise Estimation during Irreversible Electroporation Treatment through State-Space Modeling," *Bioeng.*, vol. 9, no. 10, p. 499, 2022, doi: 10.3390/bioengineering9100499.

[59] E. S. Yadav and T. Indiran, "PRBS based model identification and GPC PID control design for MIMO Process," *Mater. Today Proc.*, vol. 17, no. 1, pp. 16–25, 2019, doi: 10.1016/j.matpr.2019.06.396.

[60] G. Iadarola, P. Daponte, L. De Vito, and S. Rapuano, "On the Effects of PRBS Non-Idealities in Signal Reconstruction from AICs," *IEEE Trans. Instrum. Meas.*, vol. 72, pp. 1-11, 2023.

[61] S. Liu and Y. Chen, "Photonic Random Demodulator With Improved Performance by Compressing the PRBS Amplitude," *IEEE Photonics Technol. Lett.*, vol. 36, no. 5, pp. 329–332, 2024, doi: 10.1109/LPT.2024.3354039.

[62] D. Łuczak, "Nonlinear Identification with Constraints in Frequency Domain of Electric Direct Drive with Multi-Resonant Mechanical Part," *Energies*, vol. 14, no. 21, 2021, doi: 10.3390/en14217190.

[63] D. Walczuch, T. Nitzsche, T. Seidel, and J. Schoning, "Overview of Closed-Loop Control Systems and Artificial Intelligence Utilization in Greenhouse Farming," *2022 IEEE Int. Conf. Omni-layer Intell. Syst.*, pp. 1-6 ,2022, doi: 10.1109/COINS54846.2022.9854938.

[64] M. Schwenzer, M. Ay, T. Bergs, and D. Abel, "Review on model predictive control: an engineering perspective," *Int. J. Adv. Manuf. Technol.*, vol. 117, pp. 1327–1349, 2021, doi: 10.1007/s00170-021-07682-3.

[65] B. Verma and P. K. Padhy, "Robust Fine Tuning of Optimal PID Controller With Guaranteed Robustness," *IEEE Trans. Ind. Electron.*, vol. 67, no. 6, pp. 4911–4920, 2020, doi: 10.1109/TIE.2019.2924603.

[66] F. Niu, K. Sun, S. Huang, Y. Hu, D. Liang, and Y. Fang, "A Review on Multimotor Synchronous Control Methods," *IEEE Trans. Transp. Electrif.*, vol. 9, no. 1, pp. 22–33, 2023, doi: 10.1109/TTE.2022.3168647.

[67] A. Turan, "PID controller design with a new method based on proportional gain for cruise control system," *J. Radiat. Res. Appl. Sci.*, vol. 17, no. 1, 2024, doi: 10.1016/j.jrras.2023.100810.

[68] V. Rajs, N. L. Rašević, M. Z. Bodić, M. M. Zuković, and K. B. Babković, "PID Controller Design for Motor Speed Regulation with Linear and Non-Linear Load," *IFAC-PapersOnLine*, vol. 55, no. 4, pp. 225–229, 2022, doi: 10.1016/j.ifacol.2022.06.037.

[69] D. Debnath, P. Malla, and S. Roy, "Position control of a DC servo motor using various controllers: A comparative study," *Mater. Today Proc.*, vol. 58, no. 1, pp. 484–488, 2022, doi: 10.1016/j.matpr.2022.03.008.

[70] V. Zhmud, W. Hardt, O. Stukach, L. Dimitrov, and J. Nosek, "The Parameter Optimization of the PID and PIDD Controller for a Discrete Object," *Dyn. Syst. Mech. Mach.*, pp. 1-6, 2019, doi: 10.1109/Dynamics47113.2019.8944718.

[71] J. Fišer and P. Zítek, "PID Controller Tuning via Dominant Pole Placement in Comparison with Ziegler-Nichols Tuning," *IFAC-PapersOnLine*, vol. 52, no. 18, pp. 43–48, 2019, doi: 10.1016/j.ifacol.2019.12.204.

[72] I. A. A. Jamil and M. Moghavvemi, "Optimization of PID Controller Tuning method using Evolutionary Algorithms," *2021 Innov. Power Adv. Comput. Technol. (i-PACT)*, pp. 1–7, 2021, doi: 10.1109/i-PACT52855.2021.9696875.

[73] C. Wang, Y. Zhuang, Y. Dong, L. Zhang, L. Liu, and J. Du, "Design and control analysis of the side-stream extractive distillation column with low concentration intermediate-boiling entrainer," *Chem. Eng. Sci.*, vol. 247, 2022, doi: 10.1016/j.ces.2021.116915.

[74] J. Liu *et al.*, "Dynamic controllability strategy of reactive-extractive dividing wall column for the separation of water-containing ternary azeotropic mixture," *Sep. Purif. Technol.*, vol. 304, 2023, doi: 10.1016/j.seppur.2022.122338.

[75] T. Bestwick and K. V. Camarda, "Artificial Neural Network-Based Real-Time PID Controller Tuning," *Comput. Aided Chem. Eng. Elsevier*, vol. 52, pp. 1609–1614, 2023, doi: 10.1016/B978-0-443-15274-0.50256-0.

[76] B. M. Abubakr, O. A. Abolaeha, and A. A. Hameda, "Performance Evaluation of the Good Gain Method Against Other Methods Using a Water Level Control System," *Int. J. Syst. Appl. Eningeering Dev.*, vol. 14, 2020, doi: 10.46300/91015.2020.14.8.

[77] B. Wu, X. Han, and N. Hui, "System Identification and Controller Design of a Novel Autonomous Underwater Vehicle," *Mach.*, vol. 9, no. 6, 20121, doi: 10.3390/machines9060109.

[78] K. R. A. Govind and S. Mahapatra, "Design of PI/PID Control Algorithm for a Benchmark Heat Exchanger System using Frequency Domain Specifications," *IEEE Int. Power Renew. Energy Conf.*, pp. 1–5, 2022, doi: 10.1109/IPRECON55716.2022.10059570.

[79] L. Fan and Z. Miao, "Admittance-Based Stability Analysis: Bode Plots, Nyquist Diagrams or Eigenvalue Analysis?," *IEEE Trans. Power Syst.*, vol. 35, no. 4, pp. 3312–3315, 2020, doi: 10.1109/TPWRS.2020.2996014.

[80] G. W. Roberts, "A Modified Nyquist Stability Criteria that Takes into Account Input/Output Circuit Loading Effects," *2021 19th IEEE International New Circuits and Systems Conference (NEWCAS)*, Toulon, France, pp. 1-4, 2021, doi: 10.1109/NEWCAS50681.2021.9462771.

[81] L. Li, Y. Yu, L. Hu, X. Ruan, R. Su, and X. Fu, "Modelling and Stability Analysis for a Magnetically Levitated Slice Motor (MLSM) with Gyroscopic Effect and Non-Collocated Structure Based on the Extended Inverse Nyquist Stability Criterion," *Mach.*, vol. 9, no. 9, 2021, doi: 10.3390/machines9090201.

[82] J. Samanes *et al.*, "Control Design and Stability Analysis of Power Converters: The MIMO Generalized Bode Criterion," *IEEE J. Emerg. Sel. Top. Power Electron.*, vol. 8, no. 2, pp. 1880–1893, 2020, doi: doi: 10.1109/JESTPE.2019.2941829.

[83] S. Alghamdi, A. B. Wazir, H. H. H. Awaji, A. A. Alhussainy, H. F. Sindi, and M. Raw, "Tuning PID Controller Parameters of Automatic Voltage Regulator (AVR) Using Particle Swarm Optimization : A Comparative Study," *IEEE PES Conf. Innov. Smart Grid Technol.*, pp. 1–6, 2023, doi: 10.1109/ISGTMiddleEast56437.2023.10078497.

[84] P. Gopi, S. Srinivasan, and M. Krishnamoorthy, "Disk margin based robust stability analysis of a DC motor drive," *Eng. Sci. Technol. an Int. J.*, vol. 32, 2022, doi: 10.1016/j.jestch.2021.10.006.

[85] P. Oziablo, D. Mozyrska, and M. Wyrwas, "Discrete-Time Fractional, Variable-Order PID Controller for a Plant with Delay," *Entropy*, vol. 22, no. 7, 2020, doi: 10.3390/e22070771.

[86] A. Tsavnin, S. Efimov, and S. Zamyatin, "Overshoot Elimination for Control Systems with Parametric Uncertainty via a PID Controller," *Symmetry*, vol. 12, no. 7, 2020, doi: 10.3390/sym12071092.

[87] A. M. Abdel-hamed, A. Y. Abdelaziz, and A. El-Shahat, "Design of a 2DOF-PID Control Scheme for Frequency/Power Regulation in a Two-Area Power System Using Dragonfly Algorithm with Integral-Based Weighted Goal Objective," *Energies*, vol. 16, no. 1, 2023, doi: 10.3390/en16010486.

[88] H. Budiarto, V. Triwidyaningrum, F. Umam, and A. Dafid, "Implementation of Automatic DC Motor Braking PID Control System on (Disc Brakes)," *J. Robot. Control*, vol. 4, no. 3, 2023, doi: 10.18196/jrc.v4i3.18505.

[89] M. Y. Silaa, O. Barambones, and A. Benchérif, "A Novel Adaptive PID Controller Design for a PEM Fuel Cell Using Stochastic Gradient Descent with Momentum Enhanced by Whale Optimizer," *Electron.*, vol. 11, no. 16, 2022, doi: 10.3390/electronics11162610.

[90] R. Büchi, "PID Controller Parameter Tables for Time-Delayed Systems Optimized Using Hill-Climbing," *Signals*, vol. 3, no. 1, pp. 146–156, 2022, doi: 10.3390/signals3010010.

[91] S. S. Husain, A. Q. Al-Dujaili, A. A. Jaber, A. J. Humaidi, and R. S. Al-Azzawi, "Design of a Robust Controller Based on Barrier Function for Vehicle Steer-by-Wire Systems," *World Electr. Veh. J.*, vol. 15, no. 1, 2024, doi: 10.3390/wevj15010017.